Engineering and Applied Science Letters

PSR Press

*Article*

# Truncating the series expansion for unsteady velocity-dependent Eyring-Powell fluid

**Emran Khoshrouye Ghiasi[1,*] and Samad Noeiaghdam[2,3]**

1 Young Researchers and Elite Club, Mashhad Branch, Islamic Azad University, Mashhad, Iran.
2 South Ural State University, Lenin Prospect 76, Chelyabinsk, 454080, Russian Federation.
3 Baikal School of BTICS, Irkutsk National Research Technical University, Irkutsk, Russian Federation.
* Correspondence: khoshrou@yahoo.com

Received: 5 August 2020; Accepted: 22 October 2020; Published: 6 November 2020.

**Abstract:** The main difficulty in dealing with the basic differential equations of fluid momentum is in choosing an appropriate problem-solving methodology. In addition, it is necessary to correct minor errors incurred by neglecting some losses. However, in many cases, such methodologies suffer from long processing time (P-time). Therefore, this article focuses on the truncation technique involving an unsteady Eyring-Powell fluid towards a shrinking wall. The governing differential equations are converted to the non-dimensional from through similarity variables. It is seen that the present system is totally convergent in 8th-order approximate solution together with $\hbar = -0.875$.

**Keywords:** tHAM, P-time, square residual error, Eyring-Powell fluid, velocity distribution.

## 1. Introduction

Analyzing the rheological behavior of Eyring-Powell fluid models (at low and high shear rates), which can be easily deduced from the molecular theory of rarefied gases [1], is very important for pseudoplastic systems nowadays. Until recently, only such fluid flow problems, whether "steady" or "unsteady", have been concerned with finding the velocity and temperature distribution through the use of some particular problem-solving methodologies [2–11]. However, from a mathematical viewpoint, it can be desirable to have a series expansion which converges in the semi-infinite intervals faster than a series expansion with a smaller interval of convergence. In this way, Khoshrouye Ghiasi and Saleh [12] employed a rather convergent feature of homotopy analysis method (HAM) by adding to the truncation technique, namely, tHAM, for solving the Falkner-Skan boundary value problem (FBVP) and spotting many errors. In fact, they could give rigorous proof of their observations showing how the P-time can be minimized without any loss of accuracy. Furthermore, it is to be mentioned here that some other types of technical problems [13–29] can be solved quite simply through this starting point.

Unlike many side benefits of the truncation technique, the lack of tHAM for solving many flow problems is pronounced yet. To this aim, an efficient tHAM for studying the laminar flow velocity distribution in an Eyring-Powell fluid model subjected to inclined magnetic field is developed here. The obtained results concerning the steady case are compared and validated with those simulations available in the open literature. It is shown that the tHAM can be considered as a powerful tool for deriving high-accuracy approximations.

## 2. Problem formulation

Consider a two-dimensional unsteady laminar flow past a continuous stretching sheet of velocity $U_w = \frac{ax}{1-bt}$ where $a > 0$ and $b \geq 0$ are the initial stretching rate and unsteadiness coefficient, respectively. Here an inclined magnetic field strength $\mathcal{B}$ is applied across the conducting fluid at an acute angle $\theta$ below the free surface.

According to the Eyring-Powell fluid model, the differential equations of mass and linear momentum conservation for the assumed flow pattern can be expressed as,

$$u_{,x} + v_{,y} = 0,$$

$$\dot{u} + uu_{,x} + vv_{,y} = \left(v + \frac{1}{\rho\Gamma\Lambda}\right) u_{,yy} - \frac{1}{2\rho\Gamma\Lambda^3} u_{,y}^2 u_{,yy} - \frac{\sigma\mathcal{B}^2 sin^2\theta}{\rho} u,$$

with the boundary conditions

$$u = U_w(x,t) = \frac{ax}{1-bt} \quad , v = V(x,t) \quad \text{at} \quad y = 0,$$

$$u \to 0, \quad v \to 0, \quad \text{as} \quad y \to \infty,$$

where $v$ is the kinematic viscosity, $\rho$ is the density, $\Gamma$ and $\Lambda$ are the material constants, $\sigma$ is the electrical conductivity and $V(x,t)$ is the mass transfer rate. It is to be noted that the comma sign and dot-superscript followed by independent variables signify the partial derivative involving $\frac{\partial}{\partial x}$(or $\frac{\partial}{\partial x}$ ) and differentiation with respect to the time , respectively.

Introducing these variables $\tau = y = \sqrt{\frac{a}{v(1-bt)}}$, $u = \frac{ax}{1-bt}\varphi_{,\tau}$ and $v = -\frac{av}{1-bt}\varphi$, the governing equations and associated boundary conditions are given by

$$(1+\lambda)\varphi_{,\tau\tau\tau} - \beta(\varphi_{,\tau} + \frac{1}{2}\tau\phi_{,\tau\tau}) + \varphi\varphi_{,\tau\tau} - \varphi_{,\tau}^2 - \lambda\delta\varphi_{,\tau\tau}^2\varphi_{,\tau\tau\tau} - \mathrm{M}^2 sin^2\theta\varphi_{,\tau} = 0$$

$$\varphi = 0, \quad \varphi_{,\tau} = 1, \quad \text{at} \quad \tau = 0,$$

$$\varphi_{,\tau} = 0 \qquad \text{as} \quad \tau \to \infty,$$

where $\lambda = \frac{1}{\rho\Gamma\Lambda}$ and $\delta = \frac{a^3x^2}{2v\Lambda^2}$, are the Eyring-Powell fluid parameters, $\beta = \frac{b}{a}$ is the unsteadiness parameter and $\mathrm{M} = \sqrt{\frac{\sigma B^2}{\rho a}}$ is the magnetic field parameter.

Here the dimensionless quantity skin friction coefficient $C_f$ is defined as,

$$\sqrt{Re_x}C_f = [(1+\lambda)\varphi_{,\tau\tau}(0) - \frac{1}{3}\lambda\delta\varphi_{,\tau\tau}^3(0)],$$

where $Re_x = \frac{U_w x}{v}$ is the local Reynolds number.

## 3. Solution methodology

Let us denote the following nonlinear equation by,

$$\mathcal{N}[\varphi(\tau)] = 0,$$

where $\mathcal{N}$ is a nonlinear operator. Using $q \in [0,1]$ as an embedding parameter, the homotopy function $\mathcal{H}$ is constructed as [30]

$$\mathcal{H}(\varphi, \hat{q}, \hbar) = (1-q)\mathcal{L}[\varphi(\tau,q) - \varphi_0(\tau)] + q\hbar\mathcal{N}[\hat{\varphi}(\tau,q)], \tag{1}$$

where $\hat{\varphi}$ is an unknown function, $\hbar \neq 0$ is an auxiliary parameter, $\mathcal{L} \neq 0$ is an auxiliary linear operator and $\varphi_0$ is an initial guess of $\varphi$. It is to be noted that in the limit as approaches 0 and 1, $\hat{\varphi}(\tau,q)$ varies from the initial guess to the solution of $\varphi(\tau)$. In fact, as follows from Equation (1), $\hat{\varphi}(\tau;0) = \varphi_0(\tau)$ and $\hat{\varphi}(\tau;1) = \varphi(\tau)$ are the solution of $\mathcal{H}(\varphi;\hat{q},h)|_{q=0} = 0$ and $\mathcal{H}(\varphi;\hat{q},h)|_{q=1} = 0$, respectively. By expanding $\hat{\varphi}(\tau;q)$ n the Taylor's series with respect to, one would get

$$\hat{\varphi}(\tau;q) = \hat{\varphi}(\tau;0) + \sum_{j=1}^{\infty} \frac{1}{j!}\hat{\varphi}_{,q}^{(j)}(\tau;q)|_{q=0} = 0 = \varphi_0(\tau) + \sum_{j=1}^{\infty} \varphi_j(\tau)q^j,$$

where $\varphi_j$ is the jth-order deformation derivative. By setting $\mathcal{H}(\varphi;\hat{q},h)$ and $q$ equal to zero, the zeroth-order deformation equation is obtained as [30];

$$\mathcal{L}[\hat{\varphi}(\tau;0) - \varphi_0(\tau)] = 0.$$

By differentiating $\mathcal{H}(\varphi;\hat{q},h)$, $j$ times with respect to $q$, setting $q=0$ and dividing it by $j!$, after dropping the hats, the th-order deformation equation is constructed as

$$\mathcal{L}[\varphi_j(\tau)-x_j\varphi_{j-1}(\tau)]+\frac{1}{(j-1)!}\hbar\mathcal{N}_{,q}^{j-1}[\varphi(\tau;q)]|_{q=0}=0,$$

where

$$X_j=\begin{cases}0 & \text{if } j\leq 1,\\ 1 & \text{if } j>1.\end{cases}$$

Here the initial guess and auxiliary linear operator are taken to be

$$\varphi_0(\tau)=1-e^{-\tau},$$

$$\mathcal{L}[\varphi(\tau;q)]=\varphi_{,\tau\tau\tau}(\tau,q)-\varphi_{,q}(\tau,q),$$

with the property

$$\mathcal{L}[\alpha_1+\alpha_2e^{\tau}+\alpha_3e^{-\tau}]=0,$$

where $\alpha_1-\alpha_2$ are the integration constants. Expanding $\alpha(\tau;q)$ in the Taylor's series gives the following series expansion,

$$\alpha(\tau;q)=\varphi_0(t)+q\varphi_1(t)+q^2\varphi_2(t)+\cdots.$$

The nonlinear operator in this case is given by

$$\begin{aligned}\mathcal{N}[\alpha(t;q)] &= (1+\lambda)\varphi_{,\tau\tau\tau}(\tau,q)-\beta(\alpha_{,\tau}(\tau;q)+\frac{1}{2}\tau\varphi_{,\tau\tau}(\tau,q))-\varphi^2(\tau;q)\\ &\quad -\lambda\delta\varphi_{,\tau\tau}^2(\tau,q)\varphi_{,\tau\tau\tau}(\tau;q)-\mathcal{M}^2sin^2\theta\varphi_{,\tau}(\tau;q).\end{aligned}$$

The zeroth-order deformation equation and associated boundary conditions are written in the form

$$\varphi_{,\tau\tau\tau}(\tau)-\varphi_{0,\tau}(\tau)=0,$$

$$\varphi(\tau;q)=0,\quad \varphi_{,\tau}(\tau;q)=1\quad at\quad \tau=0,$$

$$\varphi_{,\tau}(\tau;q)\to\infty.$$

The th-order deformation equation is generated as

$$\varphi_{j,\tau\tau\tau}(\tau)-\varphi_{j,\tau}=X_j(\varphi_{j-1,\tau\tau\tau}(\tau)-\varphi_{j-1,\tau}(\tau))-\frac{1}{j-1!}\hbar\mathcal{N}_{,q}^{j-1}[\varphi(\tau,q)]|_{q=0}=0 \tag{2}$$

which goes to zero boundary conditions.

To find a more explicit way of representing the th-order deformation Equation (2), it is required to express $\frac{1}{j-1!}\hbar\mathcal{N}_{,q}^{j-1}[\varphi(\tau,q)]|_{q=0}$ by a linear combination of independent functions. With an inner product of any two independent functions in such a way that $\psi_m,\psi_n=\int_0^{\infty}(\tau)\psi_m(\tau)\psi_n(\tau)d\tau$ $m\geq 1$ and $n\leq r$ [30] where $k$ and $\tau$ are the weight function and number of truncation, respectively. The Schmidt-Gram procedure [31] as well as the Kronecker delta functions can be applied to calculate $r$. Therefore, $\frac{1}{j-1!}\hbar\mathcal{N}_{,q}^{j-1}[\varphi(\tau,q)]|_{q=0}$ will be approximated by an orthonormal set of bases $e_1,e_2,...e_r$ at each point $\tau$. It is to be noted here that after making this substitution and then solving the $p-$th order deformation Equation (2), the th-order approximate solution is achieved by

$$\varphi_p=\sum_{j=0}^{p}\varphi_j(\tau).$$

In theory, the square residual error at the th-order of approximation can be defined as [32];

$$\Delta_p=\frac{1}{d+1}\sum_{l=0}^{d}\left(\mathcal{N}\left[\sum_{z=0}^{p}\varphi_z(\tau)\right]\right)^2.$$

## 4. Results and discussion

As it was mentioned earlier, employing the tHAM for those problems lie in the semi-infinite intervals is sufficient not just for a much faster rate of convergence, but also for the less obtained P-time. To do this, the geometric and physical properties discussed in Section 2, unless stated otherwise, are given in Table 1. It is to be noted here that if the order of approximation is selected as $p = 8$, the auxiliary parameter and square residual error take the same values as before. This fact is presented in Table 2.

**Table 1.** Geometric and physical properties of the fluid.

| $\lambda$ | $\beta$ | $\delta$ | $\mathcal{M}$ | $\theta$ |
|---|---|---|---|---|
| 0.6 | $-0.5$ | 0.1 | 0.2 | $45^o$ [1ex] |

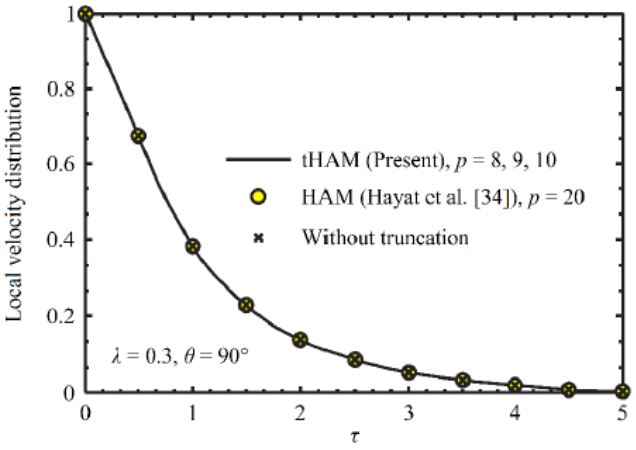


**Figure 1.** Verification of the local velocity distribution

**Table 2.** Convergence and uniqueness of the series expansion by selecting an appropriate auxiliary parameter, when the amount of P-time is rounded up to two digits.

| $p$ | $\hbar$ | $\triangle_p$ | $P-times(s)$ |
|---|---|---|---|
| 5 | $-0.864$ | $6.403 \times 10^{-9}$ | 7.41 |
| 6 | $-0.871$ | $5.179 \times 10^{-10}$ | 15.66 |
| 7 | $-0.875$ | $2.436 \times 10^{-11}$ | 32.90 |
| 8 | $-0.875$ | $2.436 \times 10^{-11}$ | 73.75 |
| 9 | $-0.875$ | $2.436 \times 10^{-11}$ | 169.15 |
| 10 | $-0.875$ | $2.436 \times 10^{-11}$ | 406.24 |

In view of the results given in Table 2, the 8th-order tHAM converges rapidly for $\hbar = -0.875$. However, due to the loop-like behavior of the tHAM, the P-time is greatly enhanced by increasing the order of approximation. According to the case reported by Zhao *et al.* [33], the main idea behind the truncation technique is to reduce the computation of series expansion and P-time made of (two or more) independent functions with a given $k$. Since the number of truncation can simply be calculated as $k = 40$ [12] therefore, the square residual error will be minimized.

**Table 3.** Skin friction coefficient vs. those geometric and physical properties

| $\lambda$ | $\beta$ | $\delta$ | $\mathcal{M}$ | $\theta$ | $[(1+\lambda)\varphi_{,\tau\tau}(0) - \frac{1}{3}\lambda\delta\varphi^3_{,\tau\tau}(0)]$ |
|---|---|---|---|---|---|
| 0.6 | $-0.5$ | 0.1 | 0.2 | $30^o$ | 1.0191 |
| 0.7 | | | | | 0.9591 |
| 0.8 | | | | | 0.9262 |
| 0.8 | $-0.4$ | | | | 0.9280 |
| | $-0.3$ | | | | 0.9516 |
| | $-0.2$ | | | | 0.9733 |
| 0.8 | $-0.2$ | 0.2 | | | 1.1170 |
| | | 0.3 | | | 1.1046 |
| | | 0.4 | | | 1.1776 |
| 0.8 | $-0.2$ | 0.4 | 0.3 | | 1.1046 |
| | | | 0.4 | | 1.1053 |
| | | | 0.5 | | 1.1061 |
| 0.8 | $-0.2$ | 0.4 | 0.5 | $45^o$ | 0.9970 |
| | | | | $60^o$ | 0.9811 |
| | | | | $90^o$ | 0.9684 |

A comparison of the local velocity distribution obtained by different solution methodologies with geometric and physical properties $\lambda = 0.3$ and $\theta = 90^o$ is shown in Figure 1. According to this Figure 1, the 8th-order tHAM gives accurate answers compared to those findings reported by Hayat *et al.* [34]; however, the order of approximation in the case analyzed by Hayat *et al.* [21] is radically different. Furthermore, the local velocity distribution for the same system without using the truncation is consistent with the tHAM results, but instead takes more P-time to consistency (i.e., 996.43s). It is worth noting that, based on the results reported in Table 2 and Figure 1, although the square residual error should be taken to optimize the value of auxiliary parameter, the only way that the P-time can reduce appears in the combination of truncation technique with the HAM.

Table 3 investigates the variation of skin friction coefficient versus different geometric and physical properties presented in Section 2. It is seen that the skin friction coefficient enhances when $\beta$, $\delta$ and $\mathcal{M}$ are increased in any case. In contrast to the previous observation, the skin friction coefficient is a diminishing function of $\theta$ and $\lambda$. Hence, one can conclude that such findings involved in Table 3 are particularly useful for developing thermodynamic characteristics of an Eyring-Powell fluid model with slip velocity at the wall.

## 5. Conclusions

Utilizing the tHAM for analyzing the unsteady Eyring-Powell fluid embedded in a shrinking wall under inclined magnetic field was the main purpose of this article. Furthermore, the square residual error at each order of approximation was minimized to accelerate the rate of convergence for the present system. It was found that the 8th-order tHAM together with $\hbar 0.875$ and $k = 40$ can give high accurate results compared to any other solution methodology simply because the P-time in this case is taken as 73.75$s$.

## 6. Nomenclature

- $u, v$ ; Velocity components along $x$ and $y$ axes, respectively $[ms^{-1}]$
- $\beta$ ; Magnetic field strength $[kgs^{-2}A^{-1}]$
- $U_w$ ; Velocity at the wall $[ms^{-1}]$
- $t$ ; time $[s]$
- $a$ ; Initial stretching rate $[a]$
- $b$ ; Unsteadiness coefficient $[b]$
- $V$ ; Mass transfer rate $[s^{-1}]$
- $\mathcal{M}$ ; Magnetic field parameter
- $C_f$ ; Skin fiction coefficient
- $Re_x$ ; Reynolds number

### Greeksymbols

- $v$ ; Kinematic viscosity $[m^2s^{-1}]$
- $\rho$ ; Density $[kgm^3]$
- $\Gamma, \Lambda$ ; Material constants
- $\sigma$ ; Electrical conductivity $[Sm^{-1}]$
- $\theta$ ; Inclined angle of magnetic field
- $\eta$ ; Similarity variable
- $\varphi$ ; Similarity function
- $\lambda, \delta$ ; Eyring-Powell fluid parameter
- $\beta$ ; Unsteadiness parameter

**Author Contributions:** All authors contributed equally to the writing of this paper. All authors read and approved the final manuscript.

**Conflicts of Interest:** "The authors declare no conflict of interest."

## References

[1] Powell, R. E., & Eyring, H. (1944). Mechanisms for the relaxation theory of viscosity. *Nature, 154*(3909), 427-428.

[2] Ogunseye, H. A., Sibanda, P., & Mondal, H. (2019). MHD mixed convective stagnation-point flow of Eyring-Powell nanofluid over stretching cylinder with thermal slip conditions. *Journal of Central South University, 26*(5), 1172-1183.

[3] Akbar, N. S., Ebaid, A., & Khan, Z. H. (2015). Numerical analysis of magnetic field effects on Eyring–Powell fluid flow towards a stretching sheet. *Journal of Magnetism and Magnetic Materials, 382*, 355-358.

[4] Hayat, T., Khan, M. I., Waqas, M., & Alsaedi, A. (2017). Effectiveness of magnetic nanoparticles in radiative flow of Eyring–Powell fluid. *Journal of Molecular Liquids, 231*, 126-133.

[5] Khan, W. A., Alshomrani, A. S., Alzahrani, A. K., Khan, M., & Irfan, M. (2018). Impact of autocatalysis chemical reaction on nonlinear radiative heat transfer of unsteady three-dimensional Eyring–Powell magneto–nanofluid flow. *Pramana, 91*(5), 1-9.

[6] Balazadeh, N., Sheikholeslami, M., Ganji, D. D., & Li, Z. (2018). Semi analytical analysis for transient Eyring-Powell squeezing flow in a stretching channel due to magnetic field using DTM. *Journal of Molecular Liquids, 260*, 30-36.

[7] Waqas, M., Khan, M. I., Hayat, T., Alsaedi, A., & Khan, M. I. (2017). On Cattaneo–Christov double diffusion impact for temperature–dependent conductivity of Powell–Eyring liquid. *Chinese Journal of physics, 55*(3), 729-737.

[8] Alshomrani, A. S., Ullah, M. Z., Capizzano, S. S., Khan, W. A., & Khan, M. (2019). Interpretation of chemical reactions and activation energy for unsteady 3D flow of Eyring–Powell magneto–nanofluid. *Arabian Journal for Science and Engineering, 44*(1), 579-589.

[9] Ramzan, M., Bilal, M., Kanwal, S., & Chung, J. D. (2017). Effects of variable thermal conductivity and non-linear thermal radiation past an Eyring Powell nanofluid flow with chemical Reaction. *Communications in Theoretical Physics, 67*(6), 723-731.

[10] Gaffar, S. A., Prasad, V. R., & Vijaya, B. (2017). Computational study of non–Newtonian Eyring–Powell fluid from a vertical porous plate with biot number effects. *Journal of the Brazilian Society of Mechanical Sciences and Engineering, 39*(7), 2747-2765.

[11] Malik, M. Y., Bilal, S., & Bibi, M. (2017). Numerical analysis for MHD thermal and solutal stratified stagnation point flow of Powell–Eyring fluid induced by cylindrical surface with dual convection and heat generation effects. *Results in physics, 7*, 482-492.

[12] Ghiasi, E. K., & Saleh, R. (2019). On approximation of FBVP by homotopy–based truncation technique. *SeMA Journal, 76*(4), 553-558.

[13] Ghiasi, E. K., & Saleh, R. (2018). Constructing analytic solutions on the Tricomi equation. *Open Physics, 16*(1), 143-148.

[14] Ghiasi, E. K., & Saleh, R. (2019). Homotopy analysis method for the Sakiadis flow of a thixotropic fluid. *The European Physical Journal Plus, 134*(1), 32.

[15] Ghiasi, E. K., & Saleh, R. (2018). Optimal homotopy asymptotic method–based Galerkin approach for solving generalized Blasius boundary value problem. *Journal of Advanced Physics, 7*(3), 408-411.

[16] Ghiasi, E. K., & Saleh, R. (2019). A convergence criterion for tangent hyperbolic fluid along a stretching wall subjected to inclined electromagnetic field. *SeMA Journal, 76*(3), 521-531.

[17] Ghiasi, E. K., & Saleh, R. (2018). Unsteady shrinking embedded horizontal sheet subjected to inclined Lorentz force and Joule heating, an analytical solution. *Results in Physics, 11*, 65-71.

[18] Ghiasi, E. K., & Saleh, R. (2018). Non-dimensional optimization of magnetohydrodynamic falkner–skan fluid flow. *INAE Letters, 3*(3), 143-147.

[19] Ghiasi, E. K., & Saleh, R. (2019). Nonlinear stability and thermomechanical analysis of hydromagnetic Falkner–Skan Casson conjugate fluid flow over an angular–geometric surface based on Buongiorno's model using homotopy analysis method and its extension. *Pramana, 92*(1),1- 12.

[20] Ghiasi, K. (2019). Emran, and Reza Saleh. "2D flow of Casson fluid with non–uniform heat source/sink and Joule heating". Front. *Heat Mass Transf, 12*, 1-7.

[21] Ghiasi, E. K., & Saleh, R. (2019). Thermophysical Investigation of Unsteady Casson–Carreau Fluid. *INAE Letters, 4*(4), 227-239.

[22] Babu, M. J., & Sandeep, N. (2017). UCM flow across a melting surface in the presence of double stratification and cross–diffusion effects. *Journal of Molecular Liquids, 232*, 27-35.

[23] Prasad, P. D., Raju, C. S. K., Varma, S. V. K., Shehzad, S. A., & Madaki, A. G. (2018). Cross diffusion and multiple slips on MHD Carreau fluid in a suspension of microorganisms over a variable thickness sheet. *Journal of the Brazilian Society of Mechanical Sciences and Engineering, 40*(5), 1-13.

[24] Sheikholeslami, M., & Rokni, H. B. (2017). Effect of melting heat transfer on nanofluid flow in existence of magnetic field considering Buongiorno Model. *Chinese Journal of Physics, 55*(4), 1115-1126.

[25] Noeiaghdam, S., Zarei, E., & Kelishami, H. B. (2016). Homotopy analysis transform method for solving Abel's integral equations of the first kind. *Ain Shams Engineering Journal, 7*(1), 483-495.

[26] Araghi, M. F., & Noeiaghdam, S. (2016). A novel technique based on the homotopy analysis method to solve the first kind Cauchy integral equations arising in the theory of airfoils. *Journal of Interpolation and Approximation in Scientific Computing, 2016*(1), 1-13.

[27] Araghi, F., & MA, N. (2018). S.: Homotopy regularization method to solve the singular Volterra integral equations of the first kind. *Jordan Journal of Mathematics and Statistics, 11*(1), 1-12.

[28] Noeiaghdam, S., Araghi, M. A. F., & Abbasbandy, S. (2019). Finding optimal convergence control parameter in the homotopy analysis method to solve integral equations based on the stochastic arithmetic. *Numerical Algorithms, 81*(1), 237-267.

[29] Noeiaghdam, S., Suleman, M., & Budak, H. (2018). Solving a modified nonlinear epidemiological model of computer viruses by homotopy analysis method. *Mathematical Sciences, 12*(3), 211-222.

[30] Liao, S. (2003). *Beyond perturbation: introduction to the homotopy analysis method*. CRC press.

[31] Weber, H. J., & Arfken, G. B. (2005). *Mathematical methods for physicists*. Elsevier Academic.

[32] Liao, S. (2010). An optimal homotopy-analysis approach for strongly nonlinear differential equations. *Communications in Nonlinear Science and Numerical Simulation, 15*(8), 2003-2016.

[33] Zhao, Y., Lin, Z., & Liao, S. (2013). An iterative HAM approach for nonlinear boundary value problems in a semi–infinite domain. *Computer Physics Communications, 184*(9), 2136-2144.

[34] Hayat, T., Ali, S., Alsaedi, A., & Alsulami, H. H. (2016). Influence of thermal radiation and Joule heating in the Eyring–Powell fluid flow with the Soret and Dufour effects. *Journal of Applied Mechanics and Technical Physics, 57*(6), 1051-1060.